IAC-21-C1.9.12

Effect of reaction wheels disbalances on the spacecraft stabilization accuracy

Yaroslav Mashtakov[a]*, Stepan Tkachev[b]

[a] *Keldysh Institute of Applied Mathematics of RAS, Space Systems Dynamics Department , Miusskaya sq. 4, Moscow, Russian Federation, 125047, yarmashtakov@gmail.com*
[b] *Keldysh Institute of Applied Mathematics of RAS, Space Systems Dynamics Department , Miusskaya sq. 4, Moscow, Russian Federation, 125047, stevens_L@mail.ru*
* Corresponding Author

Abstract

Gyroscopic attitude control systems such as reaction wheels (RW) can offer good accuracy and fast reorientation of the spacecraft. However, these systems have some drawbacks. One of them is a limited angular momentum that can be stored by RW, which leads to the necessity of additional actuators installation, e.g. magnetorquers or thrusters. The next drawback is the vibration that caused by so called disbalances. It is possible to distinguish static and dynamical disbalances. First one appears because RW center of mass does not located on its rotation axis. The dynamical disbalance is caused by misalignment of rotation axis and RW principal axis of inertia and/or asymmetry of RW tensor of inertia. Modern technologies allow us to install the set of reaction wheels even onboard small satellites, e.g. 3U or 6U Cubesats. For such kind of spacecrafts, the problem of disbalances have become more important: ratio between RW and typical Cubesat tensor of inertia grew much larger in comparison with the conventional spacecraft. Therefore, small satellites are utilized in mission that require high attitude and stabilization accuracy, e.g. for remote sensing, it is necessary to take the effect of disbalances into account. In this paper the satellite model of motion that includes both kinds of disbalances is presented. It allows us to model precise satellite motion, and demonstrates the effect of disbalances. In addition, the estimations of the attitude and stabilization accuracy that can be achieved by RW depending on the value of disbalance are presented.

Keywords: reaction wheels, imbalance, attitude accuracy

1. Introduction

Modern small satellites are able to solve many scientific and applied problems, from conducting measurements of the Earth magnetosphere to remote sensing. Most of these problems require precise satellite pointing and stabilization, which is usually provided by gyroscopic attitude control, namely by Reaction Wheels (RW). However, for such systems there is a problem of vibrations affecting the spacecraft hardware, its flexible parts and overall dynamics [1,2], which might be crucial for some missions.

One of the vibration sources is the RW imbalance. Typical angular rate of RW is several thousand rotations per minute, therefore even the small imperfections in their balancing might significantly affect the performance of the attitude control system. There are two types of imbalances that are usually distinguished. The first is the static one, which appears when the RW center of mass is not located at its rotation axis. The second is the dynamic imbalance, which corresponds to the misalignment between the RW principal axis of inertia and the rotation axis (see Figure 1). There are several approaches to deal with this problem, e.g. by installing special vibration isolation hardware [3–6]. However, such devices are unavailable for small satellites due to size and mass limitations.

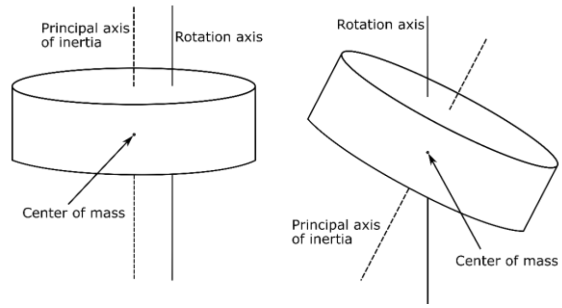

Fig. 1. RW imbalance: static (left) and dynamic (right)

Main goal of this paper is to present fully coupled model of motion for the satellite equipped with several imbalanced RWs, and provide analytical estimation of attitude and stabilization accuracy for the case of satellite inertial stabilization.

It must be noted that there are several papers that investigate the problem of RWs vibrations. For example, in [7–12] the mathematical model and experimental results of RW at suspension are presented, although these papers do not study the effect of imbalances on attitude dynamics.

The most thorough model of motion is derived in [13] which is based on the first-principle and takes into account static and dynamic imbalances. The validation of the model in [13] is carried out using kinetic energy and angular momentum conservation laws. In this paper we present similar model, which, in our opinion, might be more suitable for the software adaptation.

2. Model of motion

The spacecraft consist of the main hull with several RWs attached. The hull and each RW are supposed to be rigid bodies with known mass and inertia properties. Satellite position is described by point O – it is the arbitrary fixed point of the hull. Each reaction wheel is described by point O_k (any point of the RW rotation axis) and axis of rotation $\mathbf{e}_k$ (see Figure 2).

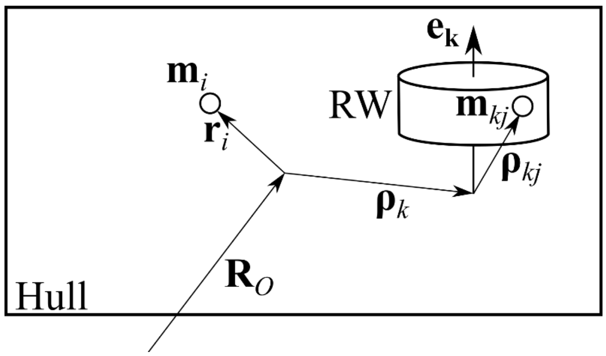

Fig. 2. Spacecraft and reaction wheel

In order to derive the equations of motion the general equation of dynamics [14] for the system with ideal constraints is used:

$$\sum_l \left(m_l \ddot{\mathbf{R}}_l - \mathbf{F}_l\right)^T \delta\mathbf{R}_l = 0 \qquad (1)$$

Here the summation is for all points of the system (for rigid bodies summation is replaced by integration), l is the system point index, m_l is the point mass, $\ddot{\mathbf{R}}_l$ is its acceleration, $\mathbf{F}_l$ is the total force affecting the point, $\delta\mathbf{R}_l$ is the point virtual displacement.

Every point of the hull $\mathbf{R}_i$ and RW $\mathbf{R}_{kj}$ is described by (see Fig.1)

$$\mathbf{R}_i = \mathbf{R}_O + \mathbf{r}_i,$$
$$\mathbf{R}_{kj} = \mathbf{R}_O + \boldsymbol{\rho}_k + \boldsymbol{\rho}_{kj},$$

where $\mathbf{R}_O$ is the satellite radius-vector, $\mathbf{r}_i$ is the vector from point O to the hull point, $\boldsymbol{\rho}_k = OO_k$, $\boldsymbol{\rho}_{kj}$ is the radius-vector from point O_k to RW point. As was mentioned earlier, O_k is the arbitrary point of RW rotation axis. It is reasonable to choose it as the projection of RW center of mass at its rotation axis. In this case, if center of mass is on rotation axis (no static imbalance) O_k represents the RW center of mass. Index i indicates the hull point and index kj indicates the j-th point of the k-th RW. Virtual displacements of the system points are

$$\delta\mathbf{R}_i = \delta\mathbf{R}_O + \delta\boldsymbol{\theta}\times\mathbf{r}_i,$$
$$\delta\mathbf{R}_{ki} = \delta\mathbf{R}_O + \boldsymbol{\delta\theta}\times\boldsymbol{\rho}_k + \left(\mathbf{e}_k\delta\varphi_k + \delta\boldsymbol{\theta}\right)\times\boldsymbol{\rho}_{kj}.$$

Here $\delta\mathbf{R}_O, \delta\boldsymbol{\theta}$ correspond to the hull virtual displacements, $\delta\varphi_k$ is the k-th RW infinitesimal rotation. Displacements $\delta\mathbf{R}_O, \delta\boldsymbol{\theta}, \delta\varphi_k$ are independent and correspond to $N = 6 + n$ system degrees of freedom (n is the RWs quantity, and 6 for translational and rotational degrees of freedom for rigid hull).

Accelerations of each satellite and RW points are

$$\begin{aligned}\ddot{\mathbf{R}}_i &= \ddot{\mathbf{R}}_O + \dot{\boldsymbol{\omega}}\times\mathbf{r}_i + \boldsymbol{\omega}\times\boldsymbol{\omega}\times\mathbf{r}_i,\\ \ddot{\mathbf{R}}_{kj} &= \ddot{\mathbf{R}}_O + \dot{\boldsymbol{\omega}}\times\boldsymbol{\rho}_k + \boldsymbol{\omega}\times\boldsymbol{\omega}\times\boldsymbol{\rho}_k\\ &\quad + \left(\dot{\boldsymbol{\omega}} + \dot{\boldsymbol{\Omega}}_k + \boldsymbol{\omega}\times\boldsymbol{\Omega}_k\right)\times\boldsymbol{\rho}_{kj}\\ &\quad + \left(\boldsymbol{\omega} + \boldsymbol{\Omega}_k\right)\times\left(\boldsymbol{\omega} + \boldsymbol{\Omega}_k\right)\times\boldsymbol{\rho}_{kj},\end{aligned}$$

where $\boldsymbol{\omega}$ is the satellite angular velocity with respect to the Inertial Frame, $\boldsymbol{\Omega}_k = \dot{\varphi}_k\mathbf{e}_k$ is the RW angular velocity with respect to the hull. Finally, (1) can be rewritten as follows:

$$\begin{aligned}&\sum_i \left(m_i\ddot{\mathbf{R}}_i - \mathbf{F}_i\right)^T \delta\mathbf{R}_i\\ &\quad + \sum_k\sum_j \left(m_{kj}\ddot{\mathbf{R}}_{kj} - \mathbf{F}_{kj}\right)^T \delta\mathbf{R}_{kj} = \sum_k M_k^{int}\delta\varphi_k\end{aligned}.$$

Here M_k^{int} is the internal torque generated in the k-th RW axis that consists of the control and friction torques. All the terms near the same virtual displacements must be equal to zero. It allows us to derive equations of motion. Detailed derivation is presented in paper [15], here we just show final expressions. Let us introduce the following notation. Cross-product matrix is

$$[\mathbf{a}]_\times := \begin{pmatrix} 0 & -a_3 & a_2 \\ a_3 & 0 & -a_1 \\ -a_2 & a_1 & 0 \end{pmatrix},$$

so $\mathbf{a}\times\mathbf{b} \equiv [\mathbf{a}]_\times \mathbf{b}$. The hull center of mass position with respect to the point O is given by

$$\mathbf{r}_s = \frac{\sum_i \mathbf{r}_i m_i}{m_s}, \quad m_s = \sum_i m_i.$$

Similarly, the center of mass of k-th RW with respect to the point O_k is

$$\boldsymbol{\rho}_{kc} = \frac{\sum_j \boldsymbol{\rho}_{kj} m_j}{m_k}, \quad m_k = \sum_j m_{kj}.$$

Since the hull point O is arbitrary, it is convenient to choose it so

$$m_s \mathbf{r}_s + \sum_k m_k \boldsymbol{\rho}_k = 0. \qquad (2)$$

Total satellite mass $m = m_s + \sum_k m_k$. Denote the hull tensor of inertia with respect to the point O

$$\mathbf{J}_s = -\sum_i [\mathbf{r}_i]_\times [\mathbf{r}_i]_\times m_i$$

and k-th RW tensor of inertia with respect to the point O_k

$$\mathbf{I}_k = -\sum_j \left[\boldsymbol{\rho}_{kj}\right]_\times \left[\boldsymbol{\rho}_{kj}\right]_\times m_{kj}$$

Total tensor of inertia of the system with respect to the point O is

$$\mathbf{J} = \mathbf{J}_s + \sum_k \mathbf{I}_k - \sum_k m_k [\boldsymbol{\rho}_k]_\times [\boldsymbol{\rho}_{kc}]_\times + m_k [\boldsymbol{\rho}_{kc}]_\times [\boldsymbol{\rho}_k]_\times + m_k [\boldsymbol{\rho}_k]_\times [\boldsymbol{\rho}_k]_\times$$

T

he total forces acting on the hull and RW are

$$\mathbf{F}_s = \sum_i \mathbf{F}_i, \ \mathbf{F}_k = \sum_j \mathbf{F}_{kj}.$$

Torques of the forces affecting RW with respect to the attachment point O_k are

$$\mathbf{M}_k = \sum_j \boldsymbol{\rho}_{kj} \times \mathbf{F}_{kj} \ .$$

Similarly, the torque affecting the hull with respect to the point O is

$$\mathbf{M}_s = \sum_i \mathbf{r}_i \times \mathbf{F}_i \ .$$

To decrease the number of brackets in the equations the following rule is used:

$$\mathbf{a}_1 \times \mathbf{a}_2 \times \ldots \times \mathbf{a}_n \equiv \mathbf{a}_1 \times \left(\mathbf{a}_2 \times \left(\ldots \times \mathbf{a}_n\right)\ldots\right).$$

Satellite dynamics is

$$\mathbf{S} \begin{pmatrix} \dot{\mathbf{V}}_O \\ \dot{\boldsymbol{\omega}} \\ \dot{\Omega}_1 \\ \vdots \\ \dot{\Omega}_n \end{pmatrix} = \mathbf{N}. \qquad (3)$$

The matrix $\mathbf{S}$ and vector $\mathbf{N}$ are defined as follows

$$\mathbf{S} = \begin{pmatrix} m\mathbf{E}_{3\times3} & -\left[\sum_k m_k \boldsymbol{\rho}_{kc}\right]_\times & -m_1 \boldsymbol{\rho}_{1c} \times \mathbf{e}_1 & \ldots & -m_n \boldsymbol{\rho}_{nc} \times \mathbf{e}_n \\ \left[\sum_k m_k \boldsymbol{\rho}_{kc}\right]_\times & \mathbf{J} & \left(\mathbf{I}_1 - m_1 [\boldsymbol{\rho}_1]_\times [\boldsymbol{\rho}_{1c}]_\times\right)\mathbf{e}_1 & \ldots & \left(\mathbf{I}_n - m_n [\boldsymbol{\rho}_n]_\times [\boldsymbol{\rho}_{nc}]_\times\right)\mathbf{e}_n \\ -\left(m_1 \boldsymbol{\rho}_{1c} \times \mathbf{e}_1\right)^T & \mathbf{e}_1^T \left(\mathbf{I}_1 - m_1 [\boldsymbol{\rho}_{1c}]_\times [\boldsymbol{\rho}_1]_\times\right) & I_1 & 0 & 0 \\ \vdots & \vdots & 0 & \ddots & 0 \\ -\left(m_n \boldsymbol{\rho}_{nc} \times \mathbf{e}_n\right)^T & \mathbf{e}_n^T \left(\mathbf{I}_n - m_n [\boldsymbol{\rho}_{nc}]_\times [\boldsymbol{\rho}_n]_\times\right) & 0 & 0 & I_n \end{pmatrix},$$

$$\mathbf{N} = \begin{pmatrix} \mathbf{F}_s + \sum_k \mathbf{F}_k - \sum_k m_k \left(\boldsymbol{\omega} \times \boldsymbol{\Omega}_k\right) \times \boldsymbol{\rho}_{kc} - \sum_k m_k \left(\boldsymbol{\omega} + \boldsymbol{\Omega}_k\right) \times \left(\boldsymbol{\omega} + \boldsymbol{\Omega}_k\right) \times \boldsymbol{\rho}_{kc} \\ \mathbf{N}_\omega \\ M_1^{int} + \mathbf{e}_1^T \mathbf{M}_1 - \mathbf{e}_1^T \left(m_1 \boldsymbol{\rho}_{1c} \times \boldsymbol{\omega} \times \boldsymbol{\omega} \times \boldsymbol{\rho}_1 + \mathbf{I}_1 \left(\boldsymbol{\omega} \times \boldsymbol{\Omega}_1\right) + \boldsymbol{\omega} \times \mathbf{I}_1 \left(\boldsymbol{\omega} + \boldsymbol{\Omega}_1\right)\right) \\ \vdots \\ M_n^{int} + \mathbf{e}_n^T \mathbf{M}_n - \mathbf{e}_n^T \left(m_n \boldsymbol{\rho}_{nc} \times \boldsymbol{\omega} \times \boldsymbol{\omega} \times \boldsymbol{\rho}_n + \mathbf{I}_n \left(\boldsymbol{\omega} \times \boldsymbol{\Omega}_n\right) + \boldsymbol{\omega} \times \mathbf{I}_n \left(\boldsymbol{\omega} + \boldsymbol{\Omega}_n\right)\right) \end{pmatrix},$$

Here

$$\begin{aligned}\mathbf{N}_\omega &= \mathbf{M}_s + \sum_k \left(\mathbf{M}_k + \boldsymbol{\rho}_k \times \mathbf{F}_k\right) - \boldsymbol{\omega}\times\mathbf{J}\boldsymbol{\omega} \\ &- \sum_k \left(\mathbf{I}_k - m_k \left[\boldsymbol{\rho}_k\right]_\times \left[\boldsymbol{\rho}_{kc}\right]_\times\right)\left(\boldsymbol{\omega}\times\boldsymbol{\Omega}_k\right) \\ &- \sum_k m_k \left(\boldsymbol{\rho}_k \times \boldsymbol{\Omega}_k \times \boldsymbol{\omega} \times \boldsymbol{\rho}_{kc} + \boldsymbol{\rho}_k \times \boldsymbol{\omega} \times \boldsymbol{\Omega}_k \times \boldsymbol{\rho}_{kc}\right. \\ &\qquad \left. + \boldsymbol{\rho}_k \times \boldsymbol{\Omega}_k \times \boldsymbol{\Omega}_k \times \boldsymbol{\rho}_{kc}\right) \\ &- \sum_k \left(\boldsymbol{\Omega}_k \times \mathbf{I}_k \boldsymbol{\omega} + \boldsymbol{\omega} \times \mathbf{I}_k \boldsymbol{\Omega}_k + \boldsymbol{\Omega}_k \times \mathbf{I}_k \boldsymbol{\Omega}_k\right).\end{aligned}$$

These equations are complemented by kinematics:

$$\begin{aligned}\dot{\mathbf{R}}_O &= \mathbf{V}_O, \\ \dot{q}_0 &= -\frac{1}{2}\mathbf{q}^T\boldsymbol{\omega}, \\ \dot{\mathbf{q}} &= \frac{1}{2}\left(q_0\boldsymbol{\omega} + \mathbf{q}\times\boldsymbol{\omega}\right), \\ \dot{\varphi}_k &= \Omega_k.\end{aligned}$$

Obtained model allows us to simulate precise motion of the satellite equipped with reaction wheels, as well as take into account possible imbalances.

3. Effect of imbalances on inertial stabilization

In this section, we analyse the effect of the imbalances in the case of inertial stabilization when the satellite is in the specific attitude with zero angular velocity. Without loss of generality let the desired attitude be the identity quaternion $\mathbf{Q}_d = \begin{pmatrix}1 & 0 & 0 & 0\end{pmatrix}^T$. All the external torques, as well as RWs friction, are neglected during the analysis. In addition, we do not consider static imbalance, i.e. RWs centers of mass are located at their rotation axes.

3.1. Effect of dynamic imbalances

The dynamic imbalance appears when RW rotation axis is misaligned with principal axis of inertia, i.e. there are nondiagonal elements in the RW tensor of inertia $\mathbf{I}_k$. The magnitude of these elements d (such that $\left|I_{kj}\right| < d$ for $k \neq j$) is usually referred as dynamic imbalance value. It is rather small in comparison with the RW axial moment of inertia I_{ax}, therefore we can introduce small parameter $\varepsilon = d/I_{ax}$. The RW tensor of inertia then is represented in the following way:

$$\mathbf{I}_k = \tilde{\mathbf{I}}_k + \varepsilon\delta\mathbf{I}_k$$

where $\varepsilon \ll 1$, $\tilde{\mathbf{I}}_k$ is nominal RW tensor of inertia such that RW rotation axis $\mathbf{e}_k$ is its axis of dynamical symmetry, $\varepsilon\delta\mathbf{I}_k$ is the imbalance additional term. Since $\tilde{\mathbf{I}}_k$ is axially symmetrical, it does not change in the Body Frame during the RW rotation. Total satellite tensor of inertia in the case of absent static imbalance (i.e. $\boldsymbol{\rho}_{kc} = 0$) is

$$\begin{aligned}\mathbf{J} &= \mathbf{J}_s + \sum_k \left(\tilde{\mathbf{I}}_k + \varepsilon\delta\mathbf{I}_k - m_k\left[\boldsymbol{\rho}_k\right]_\times\left[\boldsymbol{\rho}_k\right]_\times\right) \\ &= \tilde{\mathbf{J}} + \varepsilon\sum_k \delta\mathbf{I}_k\end{aligned}.$$

Again, here $\tilde{\mathbf{J}}$ is the nominal satellite full tensor of inertia, and $\varepsilon\sum_k \delta\mathbf{I}_k$ corresponds to the small deviations caused by imbalances.

Since we consider the case of purely dynamic imbalances, equations of motion (3) can be simplified:

$$\begin{aligned}m\ddot{\mathbf{R}}_O &= \mathbf{F}_s + \sum_k \mathbf{F}_k, \\ \mathbf{J}\dot{\boldsymbol{\omega}} &= -\boldsymbol{\omega}\times\mathbf{J}\boldsymbol{\omega} - \sum_k \mathbf{I}_k\dot{\boldsymbol{\Omega}}_k \\ &- \sum_k \left(\mathbf{I}_k\left(\boldsymbol{\omega}\times\boldsymbol{\Omega}_k\right) + \boldsymbol{\Omega}_k\times\mathbf{I}_k\boldsymbol{\omega}\right. \\ &\qquad \left. + \boldsymbol{\omega}\times\mathbf{I}_k\boldsymbol{\Omega}_k + \boldsymbol{\Omega}_k\times\mathbf{I}_k\boldsymbol{\Omega}_k\right) \\ &+ \mathbf{M}_s + \sum_k\left(\mathbf{M}_k + \boldsymbol{\rho}_k\times\mathbf{F}_k\right), \\ \mathbf{e}_k^T\mathbf{I}_k\left(\dot{\boldsymbol{\omega}} + \dot{\boldsymbol{\Omega}}_k\right) &= M_k^{int} + \mathbf{e}_k^T\mathbf{M}_k \\ &- \mathbf{e}_k^T\left(\mathbf{I}_k\left(\boldsymbol{\omega}\times\boldsymbol{\Omega}_k\right) + \left(\boldsymbol{\omega}+\boldsymbol{\Omega}_k\right)\times\mathbf{I}_k\left(\boldsymbol{\omega}+\boldsymbol{\Omega}_k\right)\right).\end{aligned}$$

We do not consider the effect of external forces and torques on attitude dynamics, therefore orbital motion might be decoupled. Hence, the system to be analysed is

$$\begin{aligned}\left(\tilde{\mathbf{J}} + \varepsilon\sum_k\delta\mathbf{I}_k\right)\dot{\boldsymbol{\omega}} + \sum_k\left(\tilde{\mathbf{I}}_k + \varepsilon\delta\mathbf{I}_k\right)\dot{\boldsymbol{\Omega}}_k &= \mathbf{a} + \varepsilon\delta\mathbf{a}, \\ \mathbf{e}_k^T\left(\tilde{\mathbf{I}}_k + \varepsilon\delta\mathbf{I}_k\right)\left(\dot{\boldsymbol{\omega}} + \dot{\boldsymbol{\Omega}}_k\right) &= b_k + \varepsilon\delta b_k,\end{aligned}$$

where

$$\begin{aligned}\mathbf{a} &= -\boldsymbol{\omega}\times\left(\tilde{\mathbf{J}}\boldsymbol{\omega} + \sum_k\tilde{\mathbf{I}}_k\boldsymbol{\Omega}_k\right), \\ \delta\mathbf{a} &= -\sum_k\left(\delta\mathbf{I}_k\left(\boldsymbol{\omega}\times\boldsymbol{\Omega}_k\right) + \left(\boldsymbol{\omega}+\boldsymbol{\Omega}_k\right)\times\delta\mathbf{I}_k\left(\boldsymbol{\omega}+\boldsymbol{\Omega}_k\right)\right) \\ b_k &= M_k^{int}, \\ \delta b_k &= -\mathbf{e}_k^T\left(\delta\mathbf{I}_k\left(\boldsymbol{\omega}\times\boldsymbol{\Omega}_k\right) + \left(\boldsymbol{\omega}+\boldsymbol{\Omega}_k\right)\times\delta\mathbf{I}_k\left(\boldsymbol{\omega}+\boldsymbol{\Omega}_k\right)\right).\end{aligned}$$

Small parameter in the left part of equations of motion might be eliminated (with the accuracy of $o(\varepsilon)$) in the following way:

$$
\begin{aligned}
&\left(\tilde{\mathbf{J}}-\sum_k \tilde{I}_k \mathbf{e}_k \mathbf{e}_k^T\right)\dot{\boldsymbol{\omega}} = \mathbf{c}+\varepsilon\delta\mathbf{c},\\
&\tilde{I}_k\dot{\Omega}_k = b_k - \tilde{I}_k \mathbf{e}_k^T\left(\tilde{\mathbf{J}}-\sum_k \tilde{I}_k \mathbf{e}_k \mathbf{e}_k^T\right)^{-1}\mathbf{c}\\
&\quad +\varepsilon\left(\delta b_k - \frac{\delta I_k}{\tilde{I}_k} b_k\right)\\
&\quad +\varepsilon\delta I_k \mathbf{e}_k^T\left(\tilde{\mathbf{J}}-\sum_k \tilde{I}_k \mathbf{e}_k \mathbf{e}_k^T\right)^{-1}\mathbf{c}\\
&\quad -\varepsilon \mathbf{e}_k^T\delta\mathbf{I}_k\left(\tilde{\mathbf{J}}-\sum_k \tilde{I}_k \mathbf{e}_k \mathbf{e}_k^T\right)^{-1}\mathbf{c}\\
&\quad -\varepsilon\tilde{I}_k \mathbf{e}_k^T\left(\tilde{\mathbf{J}}-\sum_k \tilde{I}_k \mathbf{e}_k \mathbf{e}_k^T\right)^{-1}\delta\mathbf{c}.
\end{aligned}
\tag{4}
$$

where

$$
\begin{aligned}
&\delta I_k = \mathbf{e}_k^T\delta\mathbf{I}_k\mathbf{e}_k\\
&\mathbf{c} = \mathbf{a} - \sum_k b_k\mathbf{e}_k,\\
&\delta\mathbf{c} = \delta\mathbf{a} - \sum_k\left(\delta b_k\mathbf{e}_k + b_k\left(\mathbf{E}_{3\times3} - \mathbf{e}_k\mathbf{e}_k^T\right)\frac{\delta\mathbf{I}_k\mathbf{e}_k}{\tilde{I}_k}\right)\\
&\quad -\sum_k\left(\delta\mathbf{I}_k - \delta\mathbf{I}_k\mathbf{e}_k\mathbf{e}_k^T - \mathbf{e}_k\mathbf{e}_k^T\delta\mathbf{I}_k + \mathbf{e}_k\mathbf{e}_k^T\delta I_k\right)\cdot\\
&\quad \cdot\left(\tilde{\mathbf{J}}-\sum_k \tilde{I}_k \mathbf{e}_k \mathbf{e}_k^T\right)^{-1}\left(\mathbf{a}-\sum_k b_k\mathbf{e}_k\right)
\end{aligned}
$$

Let there are n RWs with identical nominal parameters are installed onboard the spacecraft. Introduce the following matrix

$$\mathbf{A} = \left(\mathbf{e}_1, \dots, \mathbf{e}_n\right),$$

where $\mathbf{e}_k$ are the unit vectors along RWs axes of rotation. Then Lyapunov-based controller that ensures asymptotic stability of inertial stabilization is [15–17]

$$
\begin{aligned}
&\mathbf{M}_{ctrl} = -k_\omega\boldsymbol{\omega} - k_q\mathbf{q} + \boldsymbol{\omega}\times\tilde{\mathbf{J}}\boldsymbol{\omega},\\
&M_k^{int} = -\mathbf{e}_k^T\left(\mathbf{A}\mathbf{A}^T\right)^{-1}\left(\mathbf{M}_{ctrl} + \tilde{I}\boldsymbol{\omega}\times\left(\mathbf{A}\boldsymbol{\Omega}\right)\right),
\end{aligned}
\tag{5}
$$

where $\tilde{I}$ is the nominal axial moment of inertia. Since this control law ensures asymptotic stability for balanced RWs, we can expect that resulting motion would be close to the desired one. Hence, it is possible to linearize equations of motion in the vicinity of $\boldsymbol{\omega} = 0, \mathbf{q} = 0$. In this case

$$\mathbf{Q} = \begin{pmatrix} q_0 \\ \mathbf{q}\end{pmatrix} \approx \begin{pmatrix} 1 \\ \frac{1}{2}\boldsymbol{\varphi}\end{pmatrix}.$$

We will look for the solution of the system (4) under control (5) in the power series:

$$
\begin{aligned}
&\boldsymbol{\omega} = \boldsymbol{\omega}^0 + \varepsilon\boldsymbol{\omega}^1 + \dots\\
&\boldsymbol{\Omega}_k = \boldsymbol{\Omega}_k^0 + \varepsilon\boldsymbol{\Omega}_k^1 + \dots = \mathbf{e}_k\left(\Omega_k^0 + \varepsilon\Omega_k^1 + \dots\right)\\
&\mathbf{q} \approx \frac{1}{2}\left(\boldsymbol{\varphi}^0 + \varepsilon\boldsymbol{\varphi}^1 + \dots\right).
\end{aligned}
$$

After substitution in equations of motion we obtain equations of motion for zero approximation

$$
\begin{aligned}
&\left(\tilde{\mathbf{J}}-\sum_k \tilde{I}_k \mathbf{e}_k \mathbf{e}_k^T\right)\dot{\boldsymbol{\omega}}^0 = -k_\omega\boldsymbol{\omega}^0 - \frac{k_q}{2}\boldsymbol{\varphi}^0,\\
&\dot{\Omega}_k^0 = \mathbf{e}_k^T\left(\mathbf{A}\mathbf{A}^T\right)^{-1}\Bigg(k_\omega\boldsymbol{\omega}^0 + \frac{k_q}{2}\boldsymbol{\varphi}^0\\
&\qquad + \boldsymbol{\omega}^0\times\left(\tilde{\mathbf{J}}\boldsymbol{\omega}^0 + \sum_k\tilde{\mathbf{I}}_k\boldsymbol{\Omega}_k^0\right)\Bigg)\\
&\qquad + \mathbf{e}_k^T\tilde{\mathbf{I}}_k\left(\tilde{\mathbf{J}}-\sum_k \tilde{I}_k \mathbf{e}_k \mathbf{e}_k^T\right)^{-1}\left(k_\omega\boldsymbol{\omega}^0 + \frac{k_q}{2}\boldsymbol{\varphi}^0\right),
\end{aligned}
$$

and first order approximation

$$
\begin{aligned}
&\left(\tilde{\mathbf{J}}-\sum_k \tilde{I}_k \mathbf{e}_k \mathbf{e}_k^T\right)\dot{\boldsymbol{\omega}}^1 = -k_\omega\boldsymbol{\omega}^1 - \frac{k_q}{2}\boldsymbol{\varphi}^1 + \delta\mathbf{a}\big|_{\substack{\boldsymbol{\omega}=\boldsymbol{\omega}^0\\ \boldsymbol{\Omega}_k=\boldsymbol{\Omega}_k^0}}\\
&\quad -\sum_k\left(\delta b_k\big|_{\substack{\boldsymbol{\omega}=\boldsymbol{\omega}^0\\ \boldsymbol{\Omega}_k=\boldsymbol{\Omega}_k^0}}\mathbf{e}_k + b_k\big|_{\substack{\boldsymbol{\omega}=\boldsymbol{\omega}^0\\ \boldsymbol{\Omega}_k=\boldsymbol{\Omega}_k^0}}\left(\mathbf{E}_{3\times3} - \mathbf{e}_k\mathbf{e}_k^T\right)\frac{\delta\mathbf{I}_k\mathbf{e}_k}{\tilde{I}_k}\right)\\
&\quad -\sum_k\left(\delta\mathbf{I}_k - \delta\mathbf{I}_k\mathbf{e}_k\mathbf{e}_k^T - \mathbf{e}_k\mathbf{e}_k^T\delta\mathbf{I}_k + \mathbf{e}_k\mathbf{e}_k^T\delta I_k\right)\cdot\\
&\quad \cdot\left(\tilde{\mathbf{J}}-\sum_k \tilde{I}_k \mathbf{e}_k \mathbf{e}_k^T\right)^{-1}\left(-k_\omega\boldsymbol{\omega}^0 - k_q\mathbf{q}^0\right)
\end{aligned}
$$

Zero approximation has an asymptotically stable solution $\boldsymbol{\omega}^0 = \mathbf{0},\ \boldsymbol{\varphi}^0 = \mathbf{0}$. This leads to

$$
\begin{aligned}
&\delta b_k\big|_{\substack{\boldsymbol{\omega}=\boldsymbol{\omega}^0\\ \boldsymbol{\Omega}_k=\boldsymbol{\Omega}_k^0}} = 0,\quad b_k\big|_{\substack{\boldsymbol{\omega}=\boldsymbol{\omega}^0\\ \boldsymbol{\Omega}_k=\boldsymbol{\Omega}_k^0}} = 0,\\
&\delta\mathbf{a} = -\sum_k\boldsymbol{\Omega}_k^0\times\delta\mathbf{I}_k\boldsymbol{\Omega}_k^0
\end{aligned}
.
$$

In addition, from the second equation of zero approximation we can see that $\Omega_k^0 \to const$. Therefore, the equations for the first approximation are simplified

$$
\begin{aligned}
&\left(\tilde{\mathbf{J}}-\sum_k \tilde{I}_k \mathbf{e}_k \mathbf{e}_k^T\right)\dot{\boldsymbol{\omega}}^1 = -k_\omega\boldsymbol{\omega}^1 - \frac{k_q}{2}\boldsymbol{\varphi}^1\\
&\qquad -\sum_k\boldsymbol{\Omega}_k^0\times\delta\mathbf{I}_k\boldsymbol{\Omega}_k^0
\end{aligned}
\tag{6}
$$

Note that $\delta\mathbf{I}_k$ is not constant in the Body Frame since the imbalanced RWs rotate. It can be represented in the Body Frame as follows

$$\delta\mathbf{I}_k^{BF} = \mathbf{D}_k^T\delta\mathbf{I}_k^{RW}\mathbf{D}_k$$

where

$$\mathbf{D}_k = \begin{pmatrix} \cos\alpha_k & \sin\alpha_k & 0 \\ -\sin\alpha_k & \cos\alpha_k & 0 \\ 0 & 0 & 1 \end{pmatrix} \mathbf{D}_k^0, \qquad (7)$$
$$\alpha_k = \int_{t_0}^{t} \Omega_k dt + \alpha_k(t_0)$$

is the rotation matrix that corresponds to the current RW position, $\mathbf{D}_k^0$ describes the rotation from the Body Frame to the k-th RW Frame in the initial moment, $\delta\mathbf{I}_k^{RW} = const$ is the RW imbalance in k-th RW Frame. Since Ω_k^0 is constant in zero approximation, $\mathbf{D}_k$ describes constant rotation and (6) becomes the nonhomogeneous linear system of differential equations

$$\left(\tilde{\mathbf{J}} - \sum_k \tilde{I}_k \mathbf{e}_k \mathbf{e}_k^T\right)\ddot{\boldsymbol{\varphi}}^1 = -k_\omega \dot{\boldsymbol{\varphi}}^1 - \frac{k_q}{2}\boldsymbol{\varphi}^1 + \sum_k \left(\mathbf{g}_k \cos\left(t\Omega_k^0 + \alpha_k^0\right) + \mathbf{f}_k \sin\left(t\Omega_k^0 + \alpha_k^0\right)\right) \qquad (8)$$

which can be solved analytically. Note that α_k^0 is a constant initial phase. The value of the phase depends on the actual transient motion before the satellites settles near the required state. The solution of the homogeneous equation converges to zero asymptotically while the partial solution is

$$\boldsymbol{\varphi}^1 = \sum_k \left(\mathbf{u}_k \cos\left(\alpha_k^0 + \Omega_k t\right) + \mathbf{v}_k \sin\left(\alpha_k^0 + \Omega_k t\right)\right),$$

where

$$\mathbf{u}_k = -\left(\mathbf{M}^2 + \left(k_\omega \Omega_k^0\right)^2 \mathbf{E}_{3\times3}\right)^{-1}\left(k_\omega \Omega_k^0 \mathbf{f}_k + \mathbf{M}\mathbf{g}_k\right),$$
$$\mathbf{v}_k = \left(\mathbf{M}^2 + \left(k_\omega \Omega_k^0\right)^2 \mathbf{E}_{3\times3}\right)^{-1}\left(k_\omega \Omega_k^0 \mathbf{g}_k - \mathbf{M}\mathbf{f}_k\right),$$
$$\mathbf{M} = \left(\left(\tilde{\mathbf{J}} - \sum_k \tilde{I}_k \mathbf{e}_k \mathbf{e}_k^T\right)\left(\Omega_k^0\right)^2 - \frac{k_q}{2}\mathbf{E}_{3\times3}\right).$$

The angular velocity for the first approximation is

$$\boldsymbol{\omega}^1 = \sum_k \Omega_k^0 \left(-\mathbf{u}_k \sin\left(\alpha_k^0 + \Omega_k^0 t\right) + \mathbf{v}_k \cos\left(\alpha_k^0 + \Omega_k^0 t\right)\right). \qquad (9)$$

Hence the attitude stabilization error can be estimated by

$$\Delta\boldsymbol{\omega} \approx \varepsilon \sum_k \Omega_k^0 \left(-\mathbf{u}_k \sin\left(\alpha_k^0 + \Omega_k^0 t\right) + \mathbf{v}_k \cos\left(\alpha_k^0 + \Omega_k^0 t\right)\right)$$

For each i-th component then

$$\Delta\omega_i \le \varepsilon \sum_k \Omega_k^0 \sqrt{u_{ki}^2 + v_{ki}^2} \qquad (10)$$

This simple estimate might be utilized at the preliminary stage of a spacecraft design to determine the dynamic imbalance requirements for RWs. Each term in (10) is equivalent to

$$\Delta\omega_{ik} \sim \Omega_k^0 d$$

when Ω_k^0 is large enough, here d is the dynamic imbalance magnitude.

3.2. Effect of static imbalances

We apply the similar technique to the study the effect of static imbalance. Its value is usually higher than the one for the dynamic imbalance. In addition, it turns out that the stabilization accuracy in this case depends not only on the pure imbalance parameters.

Using the same approach as in the Section 3.1, the following first order approximation equations are obtained (here $\mathbf{I}_k$ are supposed to be axially symmetrical)

$$\left(\tilde{\mathbf{J}} - \sum_k \tilde{I}_k \mathbf{e}_k \mathbf{e}_k^T\right)\dot{\boldsymbol{\omega}}^1 = -k_\omega \boldsymbol{\omega}^1 - \frac{k_q}{2}\boldsymbol{\varphi}^1 - \sum_k m_k \boldsymbol{\rho}_k \times \boldsymbol{\Omega}_k^0 \times \boldsymbol{\Omega}_k^0 \times \delta\boldsymbol{\rho}_{kc} \qquad (11)$$

Here $\delta\boldsymbol{\rho}_{kc}$ represents the vector from point O_k to the RW center of mass and depends on RW rotation angle

$$\delta\boldsymbol{\rho}_{kc}^{BF} = \mathbf{D}_k \delta\boldsymbol{\rho}_{kc}^{RW},$$

where $\mathbf{D}_k$ is determined by (7). The resulting equations are similar to (8), so the resulting equations of motion are also similar.

$$\Delta\boldsymbol{\omega} \approx \rho_k \delta\rho_{kc} \sum_k \Omega_k^0 \left(-\mathbf{u}_k \sin\left(\alpha_k^0 + \Omega_k^0 t\right) + \mathbf{v}_k \cos\left(\alpha_k^0 + \Omega_k^0 t\right)\right) \qquad (12)$$

Note that attitude stabilization accuracy depends on the RW position with respect to the system center of mass $\boldsymbol{\rho}_k$, i.e. the farther RWs are placed from the system center of mass, the worse stabilization accuracy is. This result is especially useful as it allow us to reduce the effect of vibrations caused by static imbalance at the early stage of satellite design.

4. Illustrative examples

In order to show the feasibility of obtained estimations, we conduct a simulation of satellite motion. Satellite parameters are presented in Table 1. Simulation includes orbital dynamics, gravity gradient torque and RWs imbalances.

Table 1. System parameters

Parameter	Value
Hull inertia tensor, $\mathbf{J}_s$	$\mathrm{diag}\begin{pmatrix}0.027 & 0.03 & 0.01\end{pmatrix}\ \mathrm{kg}\cdot\mathrm{m}^2$
Hull mass, m_s	3.2 kg
RW static imbalance, s	$6.7\times10^{-7}\ \mathrm{kg}\cdot\mathrm{m}$
RW dynamic imbalance, d	$1.8\times10^{-9}\ \mathrm{kg}\cdot\mathrm{m}^2$
RW mass, m_k	0.119 kg
RW axis moment of inertia, I_{ax}	$1.67\times10^{-4}\ \mathrm{kg}\cdot\mathrm{m}^2$
RW equatorial moment of inertia, I_{eq}	$1.0\times10^{-4}\ \mathrm{kg}\cdot\mathrm{m}^2$
Hull inertia tensor, $\mathbf{J}_s$	$\mathrm{diag}\begin{pmatrix}0.027 & 0.03 & 0.01\end{pmatrix}\ \mathrm{kg}\cdot\mathrm{m}^2$

4.1. Dynamic imbalance

Assume that each RW tensor of inertia in its own Frame is

$$\mathbf{I}_k^{RW}=\begin{pmatrix}I_{eq} & 0 & 0\\ 0 & I_{eq} & 0\\ 0 & 0 & I_{ax}\end{pmatrix}+\Delta\mathbf{I}_k^{RW},$$

$$\Delta\mathbf{I}_k^{RW}=\begin{pmatrix}\Delta I_{11}^k & \Delta I_{12}^k & \Delta I_{13}^k\\ \Delta I_{12}^k & \Delta I_{22}^k & \Delta I_{23}^k\\ \Delta I_{13}^k & \Delta I_{23}^k & \Delta I_{33}^k\end{pmatrix},$$

where I_{eq}, I_{ax} are the RWs equatorial and axial moments of inertia (all RW nominal values are supposed to be identical). Note that $\Delta\mathbf{I}_k^{RW}$ is symmetric, and all its components are considered small with respect to the axial moment of inertia.

In RW Frame

$$\mathbf{\Omega}_k^0\times\mathbf{I}_k\mathbf{\Omega}_k^0=\left(\Omega_k^0\right)^2\begin{pmatrix}-\Delta I_{23}^k\\ \Delta I_{13}^k\\ 0\end{pmatrix}.$$

Let for all RWs $\Delta I_{13}^k=0$; and $\Delta I_{13}^k=-d$ is the dynamic imbalance. Small parameter is introduced as follows

$$\varepsilon=d/I_{ax}\ .$$

Let the nominal RWs axes of rotation coincide with $\tilde{\mathbf{J}}$ principal axes of inertia. Then in the Body Frame

$$\mathbf{\Omega}_1=\begin{pmatrix}\Omega_1 & 0 & 0\end{pmatrix}^T,$$
$$\mathbf{\Omega}_2=\begin{pmatrix}0 & \Omega_2 & 0\end{pmatrix}^T,$$
$$\mathbf{\Omega}_3=\begin{pmatrix}0 & 0 & \Omega_3\end{pmatrix}^T.$$

Matrices that describe the rotation from the RW Frame to the Body Frame are

$$\mathbf{D}_1=\begin{pmatrix}0 & 0 & 1\\ \sin\alpha_1 & \cos\alpha_1 & 0\\ -\cos\alpha_1 & \sin\alpha_1 & 0\end{pmatrix},$$

$$\mathbf{D}_2=\begin{pmatrix}\cos\alpha_2 & -\sin\alpha_2 & 0\\ 0 & 0 & 1\\ -\sin\alpha_2 & -\cos\alpha_2 & 0\end{pmatrix},$$

$$\mathbf{D}_3=\begin{pmatrix}\cos\alpha_3 & -\sin\alpha_3 & 0\\ \sin\alpha_3 & \cos\alpha_3 & 0\\ 0 & 0 & 1\end{pmatrix}.$$

Here $\alpha_k=\alpha_k^0+\Omega_k^0 t$, as in the previous section, corresponds to the current RW rotation angle. Finally, the right part of the equations (8) becomes

$$\sum_k\mathbf{\Omega}_k^0\times\delta\mathbf{I}_k\mathbf{\Omega}_k^0=\begin{pmatrix}0\\ \sin\left(\alpha_1^0+\Omega_1^0 t\right)\\ -\cos\left(\alpha_1^0+\Omega_1^0 t\right)\end{pmatrix}\left(\Omega_1^0\right)^2 I_{ax}$$
$$+\begin{pmatrix}\cos\left(\alpha_2^0+\Omega_2^0 t\right)\\ 0\\ -\sin\left(\alpha_2^0+\Omega_2^0 t\right)\end{pmatrix}\left(\Omega_2^0\right)^2 I_{ax}$$

$$+\begin{pmatrix} \cos\left(\alpha_3^0+\Omega_3^0 t\right) \\ \sin\left(\alpha_2^0+\Omega_2^0 t\right) \\ 0 \end{pmatrix}\left(\Omega_3^0\right)^2 I_{ax}.$$

In this case vectors $\mathbf{f}_k$ and $\mathbf{g}_k$ in (8) are

$$\begin{aligned} \mathbf{f}_1 &= \begin{pmatrix}0 & -1 & 0\end{pmatrix}^T \left(\Omega_1^0\right)^2 I_{ax}, \\ \mathbf{f}_2 &= \begin{pmatrix}0 & 0 & 1\end{pmatrix}^T \left(\Omega_2^0\right)^2 I_{ax}, \quad , \\ \mathbf{f}_3 &= \begin{pmatrix}0 & -1 & 0\end{pmatrix}^T \left(\Omega_3^0\right)^2 I_{ax} \end{aligned}$$

$$\begin{aligned} \mathbf{g}_1 &= \begin{pmatrix}0 & 0 & 1\end{pmatrix}^T \left(\Omega_1^0\right)^2 I_{ax}, \\ \mathbf{g}_2 &= \begin{pmatrix}-1 & 0 & 0\end{pmatrix}^T \left(\Omega_2^0\right)^2 I_{ax}, \ . \\ \mathbf{g}_3 &= \begin{pmatrix}-1 & 0 & 0\end{pmatrix}^T \left(\Omega_3^0\right)^2 I_{ax} \end{aligned}$$

For the illustration purpose consider the evolution of the angular velocity after the transient motion. So the satellite angular velocity is zero, quaternion is identical and almost all initial angular momentum is stored in the RWs. System parameters are presented in Table 1. The control parameters are $k_\omega = 0.01\ \mathrm{N\cdot m\cdot s}$, $k_a = 0.001\ \mathrm{N\cdot m}$. The results are presented in Figures 3-5. The red curves in figures are the numerical solutions, the blue curves are the approximate solutions (9), the black horizontal lines are the estimations (10). In order to test more realistic scenario, we also include gravity gradient torque into simulation. This torque is rather small, so at considerably small time spans it would not affect the results.

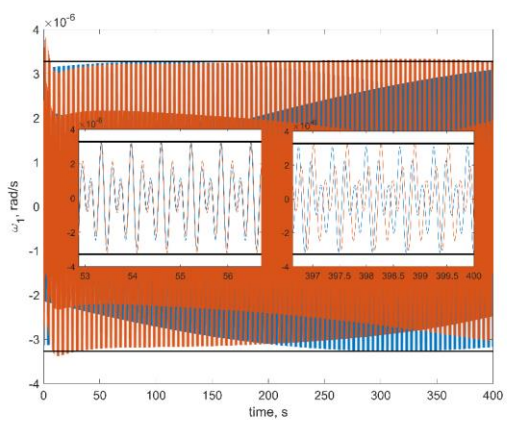

Figure 3. Evolution of ω_1 (red is numerical solution, blue is approximate solution, horizontal lines are the estimations).

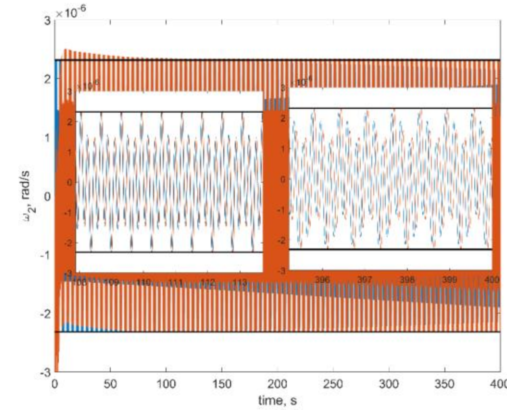

Figure 4. Evolution of ω_2 (red is numerical solution, blue is approximate solution, horizontal lines are the estimations).

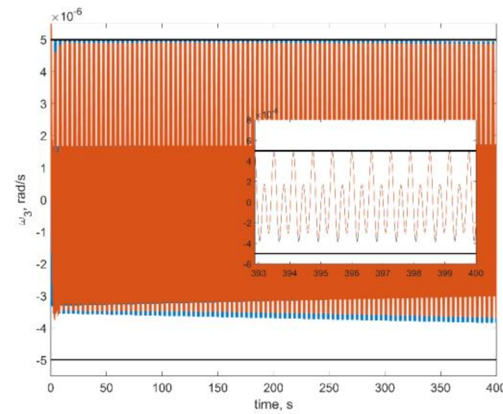

Figure 5. Evolution of ω_3 (red is numerical solution, blue is approximate solution, horizontal lines are the estimations).

First of all, one can see from figures that estimations (10) are in good accordance with the numerical simulation: numerical results are within the estimation borders, and relative difference between the linearized model of motion and the full one is around 3%. These estimations are of the utmost practical interest since these values show the stabilization accuracy of the satellite. The evolution of the angular velocity components is also close to the numerical solution. However, it should be noted that for the first and second components (Fig. 6 and 7) the phase difference increases by the end of the time interval. This is due to the non-uniform evolution of the RWs angles of rotation.

4.2. Static imbalance

Consider the same illustrative example as in the Section 3.4. The following parameters are taken additionally:

$$\boldsymbol{\rho}_1 = \begin{pmatrix} 0 & 0 & 0.01 \end{pmatrix}^T \text{ m},$$
$$\boldsymbol{\rho}_2 = \begin{pmatrix} 0.01 & 0 & 0 \end{pmatrix}^T \text{ m},$$
$$\boldsymbol{\rho}_3 = \begin{pmatrix} 0 & 0.01 & 0 \end{pmatrix}^T \text{ m},$$
$$\boldsymbol{\rho}_{kc} = \begin{pmatrix} \dfrac{s}{m_k} & 0 & 0 \end{pmatrix}^T.$$

Here s is the static imbalance, see Table 1. All other parameters are the same (without dynamic imbalance). This leads to

$$\sum_k m_k \boldsymbol{\rho}_k \times \boldsymbol{\Omega}_k^0 \times \boldsymbol{\Omega}_k^0 \times \boldsymbol{\rho}_{kc} = s\rho_1 \left(\Omega_1^0\right)^2 \begin{pmatrix} \sin\left(\alpha_1^0 + \Omega_1^0 t\right) \\ 0 \\ 0 \end{pmatrix} + s\rho_2 \left(\Omega_2^0\right)^2 \begin{pmatrix} 0 \\ -\sin\left(\alpha_2^0 + \Omega_2^0 t\right) \\ 0 \end{pmatrix} + s\rho_3 \left(\Omega_3^0\right)^2 \begin{pmatrix} 0 \\ 0 \\ \cos\left(\alpha_2^0 + \Omega_2^0 t\right) \end{pmatrix}.$$

In this case vector $\mathbf{f}_k$ and $\mathbf{g}_k$ in (8) are

$$\mathbf{f}_1 = \begin{pmatrix} -1 & 0 & 0 \end{pmatrix}^T \left(\Omega_1^0\right)^2 s\rho_1,$$
$$\mathbf{f}_2 = \begin{pmatrix} 0 & 1 & 0 \end{pmatrix}^T \left(\Omega_2^0\right)^2 s\rho_2, \quad ,$$
$$\mathbf{f}_3 = \begin{pmatrix} 0 & 0 & 0 \end{pmatrix}^T,$$

$$\mathbf{g}_1 = \begin{pmatrix} 0 & 0 & 0 \end{pmatrix}^T,$$
$$\mathbf{g}_2 = \begin{pmatrix} 0 & 0 & 0 \end{pmatrix}^T, \quad .$$
$$\mathbf{g}_3 = \begin{pmatrix} 0 & 0 & -1 \end{pmatrix}^T \left(\Omega_3^0\right)^2 s\rho_3.$$

The results of illustrative numerical simulation are presented in Figures 6-8. Black lines are the analytical estimations, red and blue lines are the numerical simulation results.

The example shows that the expressions (12) are in a good accordance with numerical simulations. As we can see from insertions, the difference between analytical estimations and numerical simulation results is rather small and lies in the worst case within 5%. The difference can be explained by the gravity gradient torque which is included in the numerical model but is not taken into account in the analytical study.

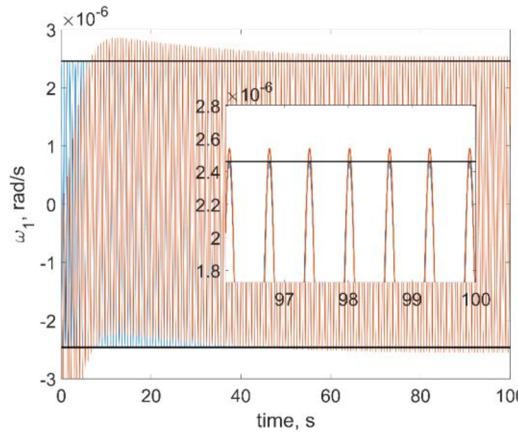

Fig. 6. Evolution of ω_1 for static imbalance case (red is numerical solution, blue is approximate solution, horizontal lines are the estimations)

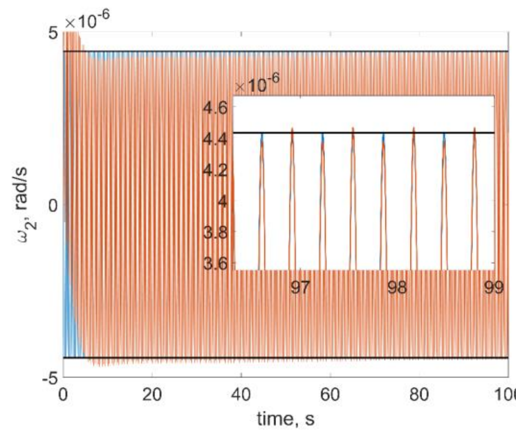

Fig. 7. Evolution of ω_2 for static imbalance case (red is numerical solution, blue is approximate solution, horizontal lines are the estimations)

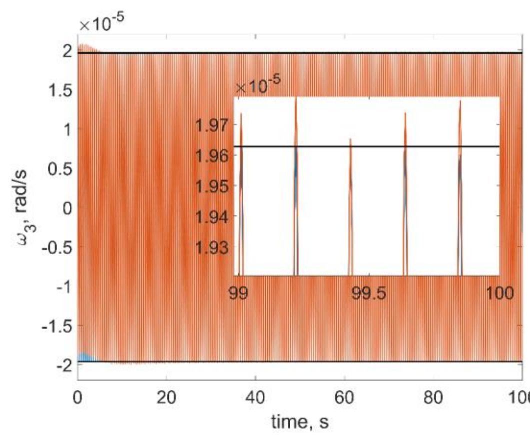

Fig. 8. Evolution of ω_3 for static imbalance case (red is numerical solution, blue is approximate solution, horizontal lines are the estimations)

As one can see, both dynamic and static imbalances lead to the additional terms in the right parts of (8) and (11), which do not depend on satellite state vector components for the first order approximation, so the total stabilization accuracy is the sum of (9) and (12).

5. Conclusion

In the paper the satellite motion analysis is carried out. The model includes RWs static and dynamic imbalances and couples orbital and angular satellite motion with RW rotation. Software implementation of the model is validated using the momentum, angular momentum, and kinetic energy conservation laws. The simulations show that the integration step should be rather small due to the high values of typical RW angular velocities. This fact makes purely numerical analysis difficult. In order to solve this problem, the analytical approximations for the satellite stabilization accuracy are obtained in closed form for the static and dynamic imbalances presence in the inertial stabilization case. The comparison of the numerical simulation and approximate solution shows that they are in a good accordance (relative error is about several percent). The explicit expressions can easily be implemented and are useful during the preliminary satellite design stage.

The estimations of the attitude accuracy are obtained for the case of the satellite Inertial Stabilization. The case of Orbital Stabilization is the main goal of future research.

Acknowledgements

This work is supported by Russian Science Foundation (grant no. 17-71-20117)

References

[1] L.M. Elias, D.W. Miller, A coupled disturbance analysis method using dynamic mass measurement techniques, Collect. Tech. Pap. - AIAA/ASME/ASCE/AHS/ASC Struct. Struct. Dyn. Mater. Conf. 1 (2002) 401–412. https://doi.org/10.2514/6.2002-1252.

[2] M. Remedia, G.S. Aglietti, G. Richardson, M. Sweeting, Integrated semiempirical methodology for microvibration prediction, AIAA J. 53 (2015) 1236–1250. https://doi.org/10.2514/1.J053339.

[3] D.-O. Lee, G. Park, J.-H. Han, Hybrid isolation of micro vibrations induced by reaction wheels, J. Sound Vib. 363 (2016) 1–17. https://doi.org/10.1016/j.jsv.2015.10.023.

[4] Y. Zhang, Z. Guo, H. He, J. Zhang, M. Liu, Z. Zhou, A novel vibration isolation system for reaction wheel on space telescopes, Acta Astronaut. 102 (2014) 1–13. https://doi.org/10.1016/j.actaastro.2014.05.014.

[5] Y. Kong, H. Huang, Vibration isolation and dual-stage actuation pointing system for space precision payloads, Acta Astronaut. 143 (2018) 183–192. https://doi.org/10.1016/j.actaastro.2017.11.038.

[6] Q. Luo, D. Li, J. Jiang, Analysis and optimization of microvibration isolation for multiple flywheel systems of spacecraft, AIAA J. 54 (2016) 1719–1731. https://doi.org/10.2514/1.J053885.

[7] M.P. Le, M.H.M. Ellenbroek, R. Seiler, P. van Put, E.J.E. Cottaar, A Full Disturbance Model for Reaction Wheels, ASME 2014 Int. Des. Eng. Tech. Conf. Comput. Inf. Eng. Conf. – Am. Soc. Mech. Eng. Digit. Collect. (2014). https://doi.org/10.1115/DETC2014-34480.

[8] H. Alkomy, J. Shan, Modeling and validation of reaction wheel micro-vibrations considering imbalances and bearing disturbances, J. Sound Vib. 492 (2021) 115766. https://doi.org/10.1016/j.jsv.2020.115766.

[9] W. Zhou, D. Li, Q. Luo, K. Liu, Analysis and Testing of Microvibrations Produced by Momentum Wheel Assemblies, Chinese J. Aeronaut. 25 (2012) 640–649. https://doi.org/10.1016/S1000-9361(11)60430-5.

[10] D. Addari, G.S. Aglietti, M. Remedia, Experimental and numerical investigation of coupled microvibration dynamics for satellite reaction wheels, J. Sound Vib. 386 (2017) 225–241. https://doi.org/10.1016/j.jsv.2016.10.003.

[11] Z. Zhang, G.S. Aglietti, W. Zhou, Microvibrations induced by a cantilevered wheel assembly with a soft-suspension system, AIAA J. 49 (2011) 1067–1079. https://doi.org/10.2514/1.J050791.

[12] D. Addari, G.S. Aglietti, M. Remedia, Dynamic mass of a reaction wheel including gyroscopic effects: An experimental approach, AIAA J. 55 (2017) 274–285. https://doi.org/10.2514/1.J055398.

[13] J. Alcorn, C. Allard, H. Schaub, Fully Coupled Reaction Wheel Static and Dynamic Imbalance for Spacecraft Jitter Modeling, J. Guid. Control. Dyn. 41 (2018) 1380–1388. https://doi.org/10.2514/1.G003277.

[14] F. Gantmacher, Lectures in Analytical

Mechanics, Mir Publishers, 1975.

[15] S. Tkachev, Y. Mashtakov, D. Ivanov, D. Roldugin, M. Ovchinnikov, Effect of reaction wheel imbalances on attitude and stabilization accuracy, Aerospace. 8 (2021). https://doi.org/10.3390/aerospace8090252.

[16] P. Tsiotras, New Control Laws for the Attitude Stabilization of Rigid Bodies, in: 13th IFAC Symp. Autom. Control Aerosp., 1994: pp. 316–321. https://doi.org/10.1016/B978-0-08-042238-1.50054-9.

[17] B. Wie, P.M. Barba, Quaternion feedback for spacecraft large angle maneuvers, J. Guid. Control. Dyn. 8 (1985) 360–365. https://doi.org/10.2514/3.19988.